

# Is this normal? A new projection pursuit index to assess a sample against a multivariate null distribution

Annalisa Calvi

School of Mathematics, Monash University

and

Ursula Laa

Institute of Statistics, University of Natural Resources and Life Sciences, Vienna

and

Dianne Cook

Department of Econometrics and Business Statistics, Monash University

July 16, 2024

## Abstract

Many data problems contain some reference or normal conditions, upon which to compare newly collected data. This scenario occurs in data collected as part of clinical trials to detect adverse events, and or for measuring climate change against historical norms. The data is typically multivariate, and often the normal ranges are specified by a multivariate normal distribution. The work presented in this paper develops methods to compare the new sample against the reference distribution with high-dimensional visualisation. It uses a projection pursuit guided tour to produce a sequence of low-dimensional projections steered towards those where the new sample is most different from the reference. A new projection pursuit index is defined, and the drawing of the projected ellipse is computed analytically. The methods are implemented in the R package, `tourr`.

*Keywords:* exploratory data analysis, statistical graphics, dimension reduction, high-dimensional visualisation, climate change, clinical trials

# 1 Introduction

Linear projections are useful in many aspects of statistical analysis of multivariate data, and especially useful for visualising the data. A linear projection provides a dimension reduction while maintaining interpretability. For example, a biplot ([Gabriel 1971](#), [Gower & Hand 1996](#)) shows the structure creating the maximum variance in the data, and also visualizing the projection matrix to learn which variables contribute to it. We might find clusters of outliers that were hiding in high dimensions.

More generally, projection pursuit ([Friedman & Tukey 1974](#), [Jones & Sibson 1987](#), [Huber 1985](#)) defines a quantitative criterion for the interestingness of a projection (a projection pursuit index), and searches the space of possible projections for the most interesting one to display. We can also define sequences of interpolated linear projections to better understand a multivariate distribution. Animating a randomly selected interpolated sequence of linear projections is called a grand tour ([Asimov 1985](#), [Buja & Asimov 1986](#), [Buja et al. 2005](#), [Cook et al. 2006](#), [Lee et al. 2022](#)). The combination of these two approaches would then use a projection pursuit index to select interesting projections, but display them via an interpolated path to provide context. This is called a guided tour ([Cook et al. 1995](#)).

The question is whether we can use these techniques to assess new data samples in the context of an established normal, such as a specific multivariate normal distribution. In physics, the normal distribution may describe experimental results, or a global fit for a selected model, and we might want to compare to a set of other models. In medical applications, the normal distribution might summarize historic data of a healthy population and we compare it to samples from new patients. In outlier detection we might use robust measures to define the normal distribution and look for anomalies.

This paper describes a new projection pursuit index which is optimized by projections where a new sample is most distant from the existing normal distribution. It is organised as follows. Section 2 provides more context for the methods and visualisation. Section 3 provides the details of the new index, and example use is illustrated in Section 5.

## 2 Background

To compare a new sample with an existing norm, like a multivariate normal distribution, in higher than two dimensions, we have typically used two samples of points. The norm is represented by points on the surface of a  $p$ -dimensional ellipsoid, corresponding to a confidence level. A sample of points uniformly distributed on a  $p$ -dimensional sphere is generated by

1. Simulating a sample of observations ( $\mathbf{x}$ , which are  $p$ -D vectors) from  $N_p(\boldsymbol{\mu}, \Sigma)$ .
2. Transforming each observation to have unit distance from the mean,  $\frac{\mathbf{x}^\top}{\|\mathbf{x}^\top\|}$ . To convert this to points on the surface of a confidence ellipsoid,
3. transform the shape using a specific variance covariance, and shift to center on the mean vector.

Finally, new observations can be visually compared with this ellipsoid by

4. plotting them together.

Figure 1 illustrates this process for 2-D. This is easiest way to view this normal region relative to a new sample for any  $p$ -D problem.

For example, Figure 2 compares a new sample of patient scores against the normal range represented by an ellipse (a) and also against a simulated sample of normal patients (b).

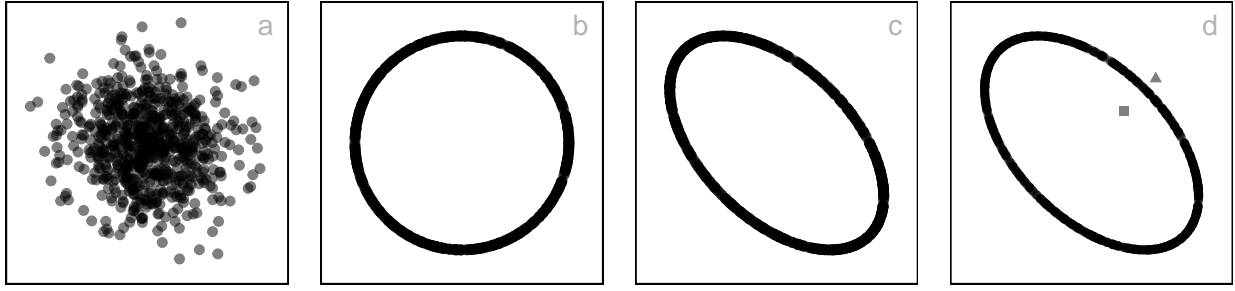


Figure 1: Simulating a uniform sample on a sphere involves sampling from a multivariate normal (a) and transforming each observation to have length equal to 1 (b). A confidence ellipsoid is generated by transforming the sphere relative to a specified variance-covariance matrix (c), and new observations can be visually assessed to be inside or outside by plotting with the ellipsoid (d).

While these are useful approaches, the ragged edges of the projected ellipse make it difficult to compare the new sample precisely against the normal ranges.

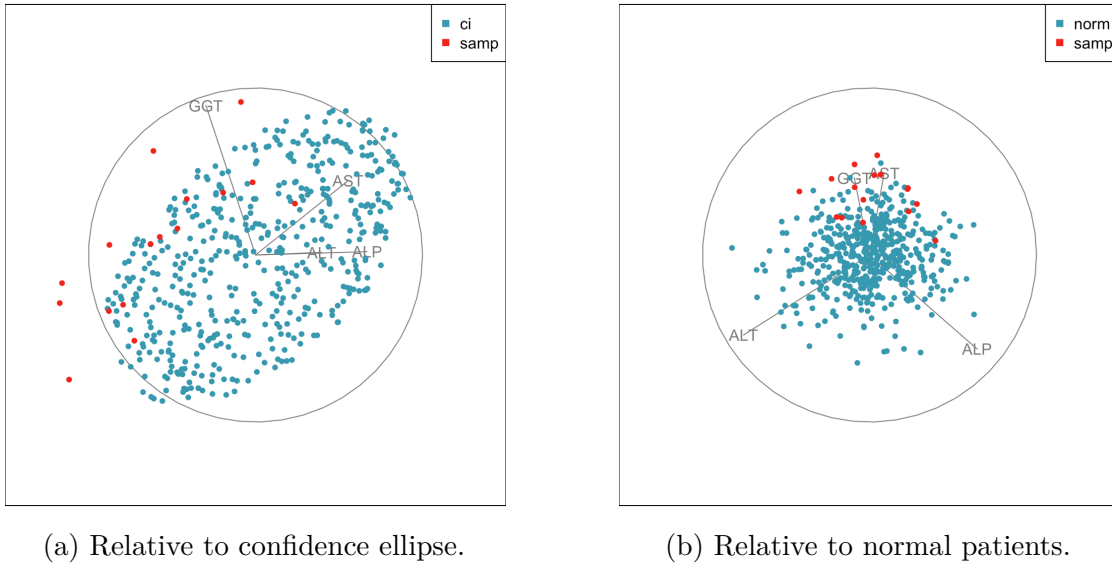


Figure 2: Illustration of current procedure: (a) compare new sample with points of the surface of a  $p$ - $D$  ellipse, (b) compare new sample with a simulated sample of normal patients. Although both approaches are useful, the rough edges of the projected ellipse points makes it difficult to precisely assess the positions of the new sample against the normal bounds.

Although this is flexible, this does not make it easy to guide the tour towards the directions (projections) where the samples are most different from the normal. What would be desirable is to analytically define the confidence ellipsoid, flag observations that are outside, steer the tour to projections that reveal the extent of the difference. And also display the

projected ellipsoid as a geometric shape rather than a sample of points. These are the procedures that are described in the next section.

### 3 Anomaly index

#### 3.1 Projecting an ellipsoid

A  $p$ - $D$  ellipsoid corresponding to a given variance-covariance ( $\Sigma$ ) is defined by

$$(\mathbf{x} - \boldsymbol{\mu})\Sigma^{-1}(\mathbf{x} - \boldsymbol{\mu})^T = c^2$$

where  $c$  a constant that depends on a specific confidence level.

**Theorem.** *The projection of this  $p$ - $D$  ellipsoid in 2- $D$  has the equation*

$$(\mathbf{y} - \boldsymbol{\mu}_p)(P^T\Sigma P)^{-1}(\mathbf{y} - \boldsymbol{\mu}_p)^T = c^2.$$

*Proof.* The projection of an ellipsoid onto 2- $D$  is an ellipse, where the curve of the ellipse is defined through the set of points  $\mathbf{x}$  for which the gradient is parallel to the projection plane. That is, the curve consists of  $\mathbf{x}$  satisfying

$$\nabla(\mathbf{x} - \boldsymbol{\mu})\Sigma^{-1}(\mathbf{x} - \boldsymbol{\mu})^T = 2(\mathbf{x} - \boldsymbol{\mu})\Sigma^{-1} = 2\mathbf{s}P^T$$

for some  $\mathbf{s} \in \mathbb{R}^2$ , where  $P$  is a  $(p \times 2)$  orthonormal basis defining the projection. We can write  $\mathbf{x} - \boldsymbol{\mu} = \mathbf{s}P^T\Sigma$ . Making this substitution in the  $p$ - $D$  ellipsoid equation yields

$$c^2 = (\mathbf{x} - \boldsymbol{\mu})\Sigma^{-1}(\mathbf{x} - \boldsymbol{\mu})^T = \mathbf{s}P^T\Sigma P\mathbf{s}^T$$

We call points in the projection that are on the curve  $\mathbf{y}$ , so that  $\mathbf{y} = \mathbf{x}P$  for  $\mathbf{x}$  on the  $p$ - $D$  curve. Then  $\mathbf{y} - \boldsymbol{\mu}_p = (\mathbf{x} - \boldsymbol{\mu})P = \mathbf{s}P^T\Sigma P$ , where  $\boldsymbol{\mu}_p = \boldsymbol{\mu}P$  is the projected mean. We then substitute  $(\mathbf{y} - \boldsymbol{\mu}_p)(P^T\Sigma P)^{-1}$  for  $\mathbf{s}$  in the equation  $c^2 = \mathbf{s}P^T\Sigma P\mathbf{s}^T$ . From this we can compute the analog equation for the projection as

$$(\mathbf{y} - \boldsymbol{\mu}_p)(P^T\Sigma P)^{-1}(\mathbf{y} - \boldsymbol{\mu}_p)^T = c^2$$

as claimed. □

This means the matrix  $(P^T\Sigma P)^{-1}$  is defining the ellipse in the 2- $D$  projection. In general  $c$  could be any constant, but typically we would select it as a quantile of the  $\chi^2$  distribution, so that the size of the ellipse corresponds to a selected probability.

### 3.2 Index specification

To define a measure of an interesting projection is to maximize the average Mahalanobis distance ([Mahalanobis 1936](#)) in the projection for a subset of points,  $W$ . The set of points could be chosen in different ways, but the default is those that are outside the specified ellipsoid in  $p$ - $D$ . Alternatives could be to select a set of observations with the largest Mahalanobis distance, manually select observations or possibly a group of points identified via clustering of the extremes.

The index is written as

$$\sum_{\mathbf{w} \in W} (\mathbf{w} - \boldsymbol{\mu}) P (P^T \Sigma P)^{-1} P^T (\mathbf{w} - \boldsymbol{\mu})^T$$

where by default  $W = \{\mathbf{x} : (\mathbf{x} - \boldsymbol{\mu}) \Sigma^{-1} (\mathbf{x} - \boldsymbol{\mu})^T > c^2\}$ , is the set of observations outside the  $p$ - $D$  ellipsoid.

### 3.3 Additional considerations

If the observations in  $W$  are primarily departing from the normal range in the same direction, the index will be expected to perform well in finding this average direction. However, if the observations have very different departures from the norm, it may be useful to break them into groups, and separately optimize on these subsets. One could consider clustering these observations using angular distance to find groups of observations that have similar directions of departure.

## 4 Implementation

This is implemented in the `tourr` (Wickham et al. 2011, 2024) package, where the projected ellipsoid can be drawn for each projection. The guided tour will take arguments specifying the data, and the null variance-covariance matrix.

```
library(tourr)

animate_xy(samp, guided_anomaly_tour(anomaly_index(),
  ellipse=vc_null), ellipse=vc_null,
  axes = "bottomleft", half_range=5, center=FALSE)
```

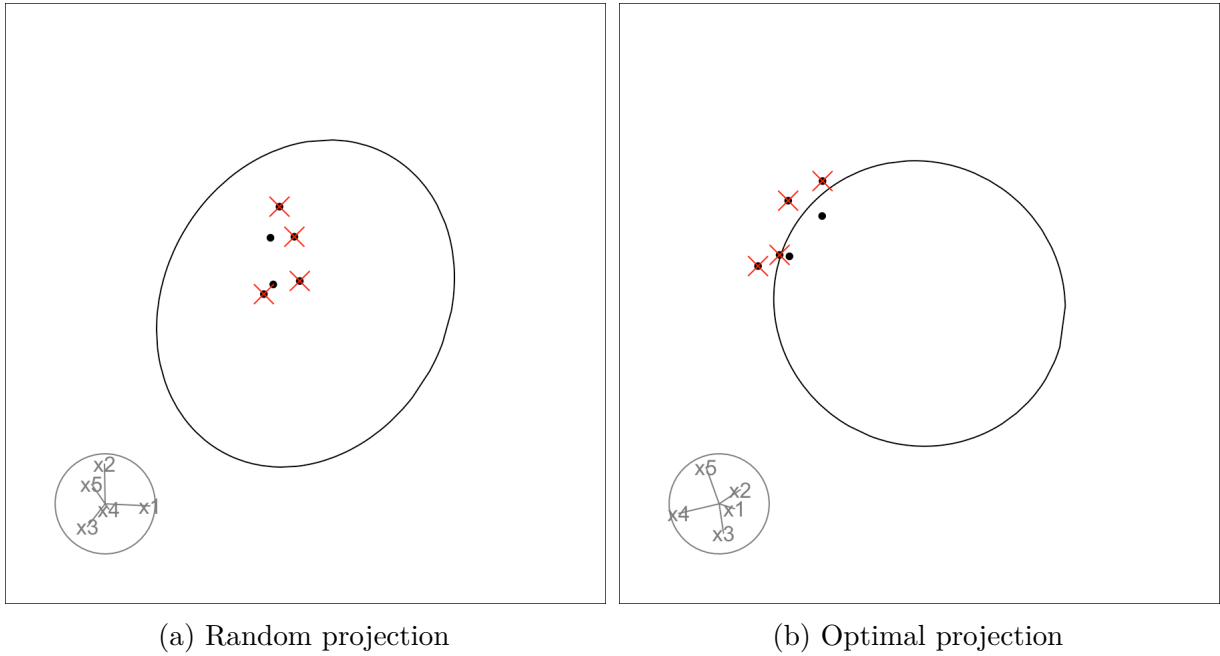


Figure 3: Two projections of simulated example data corresponding to the sample code: (a) random projection where sample is inside the 2-D ellipse, (b) optimal projection from index, showing most of the sample outside. A red cross indicates that the point is outside the p-D ellipse. The optimal projection uses mostly variables  $x_4, x_5$ , which is expected because these are the two directions where the sample most differs from the norm.

## 5 Examples

### 5.1 Health: liver function tests

This example is motivated by a problem posed during consulting with a pharmaceutical company, but the data shown here is simulated, simply to illustrate the application. Liver function tests commonly provide measurements on albumin, protein, bilirubin, gamma-glutamyl- transferase (GGT), aspartate aminotransferase (AST), alkaline phosphatase (ALP) and alanine aminotransferase (ALT). There are normal ranges on these measurements reported by [Lala et al. \(2023\)](#) and listed in Table 1.



Table 1: Normal ranges provided for liver function tests.

	albumin	protein	bilirubin	GGT	AST	ALP	ALT
	(g/L)	(g/L)	( $\mu$ mol/L)	(IU/L)	(IU/L)	(IU/L)	(IU/L)
min	35	60	0	2	5	30	5
max	50	80	20	44	30	120	40

These measurements are also likely correlated, based on guidance like the *ratio of AST to ALT of 2:1 indicates possible alcohol abuse*. Although this was provided by the pharmaceutical company, correlation between these measurements for normal patients is not readily available. When a correlation matrix for normal patients is provided this would allow construction of the null ellipse upon which to examine new samples.

Figure 4 illustrates two examples. The first is similar to the consulting project. A sample of liver test scores for new patients was provided in order to examine their values relative to the normal range. Here only four tests are used, GGT, AST, ALP, ALT. Plot (a) shows a projection of this sample relative to the normal range. Three of the patients are outside the confidence ellipse but all of the patients are located away from the mean. What has been typical in the past is to compute normal values based on tests of healthy young males. The samples provided for the project were all recorded on women. We see that this sample has slightly lower ALT and ALP, which is consistent with what is reported in [Lala et al. \(2023\)](#).

The second example shows a longitudinal record of a single patient, measured at ages 45, 50, 55, 65 and 70. The lines connect the records in time order. The projection corresponds to the maximum from a projection-pursuit guided tour using the anomaly index:

$$P = \begin{bmatrix} 0.371 & -0.128 \\ -0.388 & 0.732 \\ 0.140 & 0.599 \\ -0.832 & -0.297 \end{bmatrix}$$

From the axes representation in Figure 4 (b) of this projection, we can see that the direction that profile extends is primarily contrasting ALT (fourth row) and ALP (third row). This is consistent with aging, where ALP increases and ALT decreases.

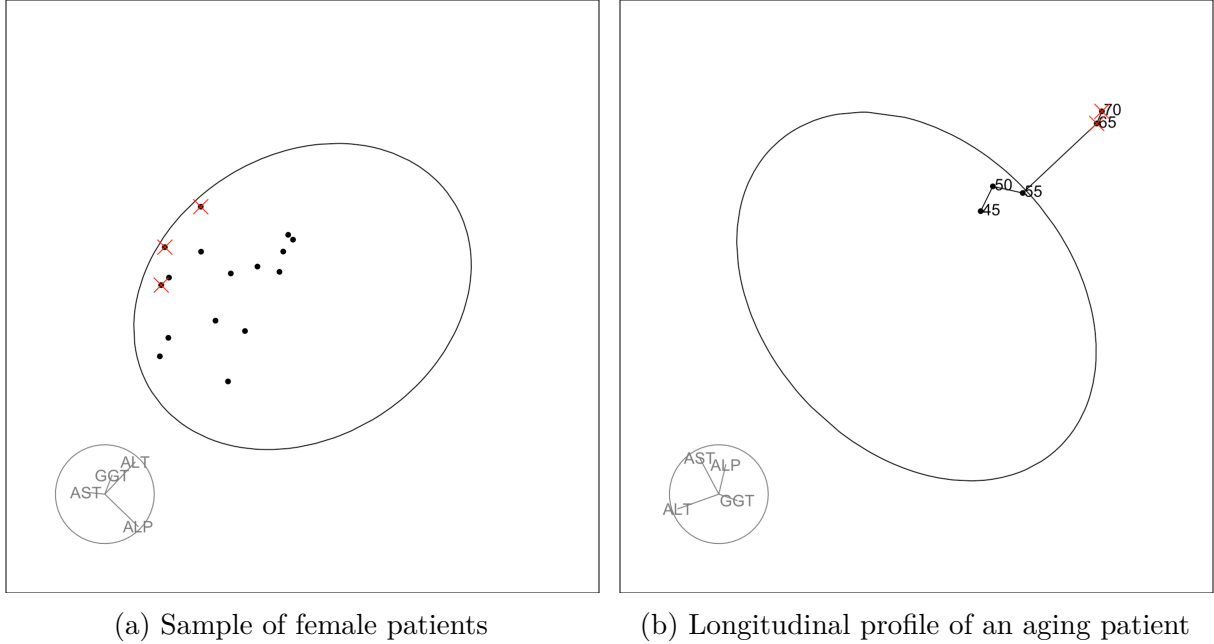


Figure 4: Two projections of simulated example data corresponding to common liver tests: (a) sample of female patients, (b) longitudinal test results for a single patient. Red cross indicates observation is outside the 4-D confidence ellipse. The female patients tend to have lower ALP and ALT than the normal range. As the patient ages, the level of ALP increases and ALT decreases.

## 5.2 Robust statistics: weather extremes

This example is motivated by the weather data example from [Filzmoser et al. \(2018\)](#). We illustrate using the anomaly index to compare potential outliers with a reference normal

distribution that is derived using robust methods on the original data. The data contains 16 numerical measurements that are averages across the three summer months June, July and August, reported for 68 years (1955 - 2022) (see [Filzmoser et al. \(2018\)](#) for more details).

To estimate the underlying normal distribution the data is first centered and scaled using the median and the median absolute deviation (MAD), before applying the minimum covariance determinant (MCD) estimator ([Rousseeuw 1985](#)) using the implementation in [Maechler et al. \(2024\)](#). The MCD estimates for the mean vector and the variance-covariance matrix are then used to define the reference normal distribution.

Here we will consider points to be outlying if they are more than  $5\sigma$  away from that mean value. With  $p = 16$  this corresponds to a Mahalanobis distance of 60 or larger. This will identify 20 out of the 68 observations as outlying. Since these are outlying in different combinations of variables, as found in [Filzmoser et al. \(2018\)](#), we will further separate the outlying points into clusters based on similarity in direction. The similarity is computed by first normalizing observations to have length 1 and then apply k-means clustering with Euclidean distance. We use the Dunn index [Halkidi et al. \(2002\)](#), computed using [Hennig \(2024\)](#), to select the preferred number of clusters,  $k = 5$ .

The new anomaly index is first applied to the full dataset, such that the final projection will be affected by averaging distance of points in many directions, see Figure 5 (a). It provides a global picture showing where the outlying points differ from the normal distribution. We can see that the contrast between maximum (atmx) and minimum (atmn) temperature is primarily used in the direction where points are most outlying. In the orthogonal direction the variables precipitation (prc) and number of days with maximum temperature above 25°C (nsm) can be used to separate the clusters 2, 3 and 5. With this solution the two points in cluster 4 cannot be resolved, they fall inside the ellipse. To better understand

what is different for those two years we separately run the anomaly index for this subset, see Figure 5 (b). From the result we see that the maximum temperature is not relevant for this cluster, but that they have low values for the minimum temperature. We also see that there is still some averaging, and the preferred solution is not placing either point on the outside of the projected ellipse.

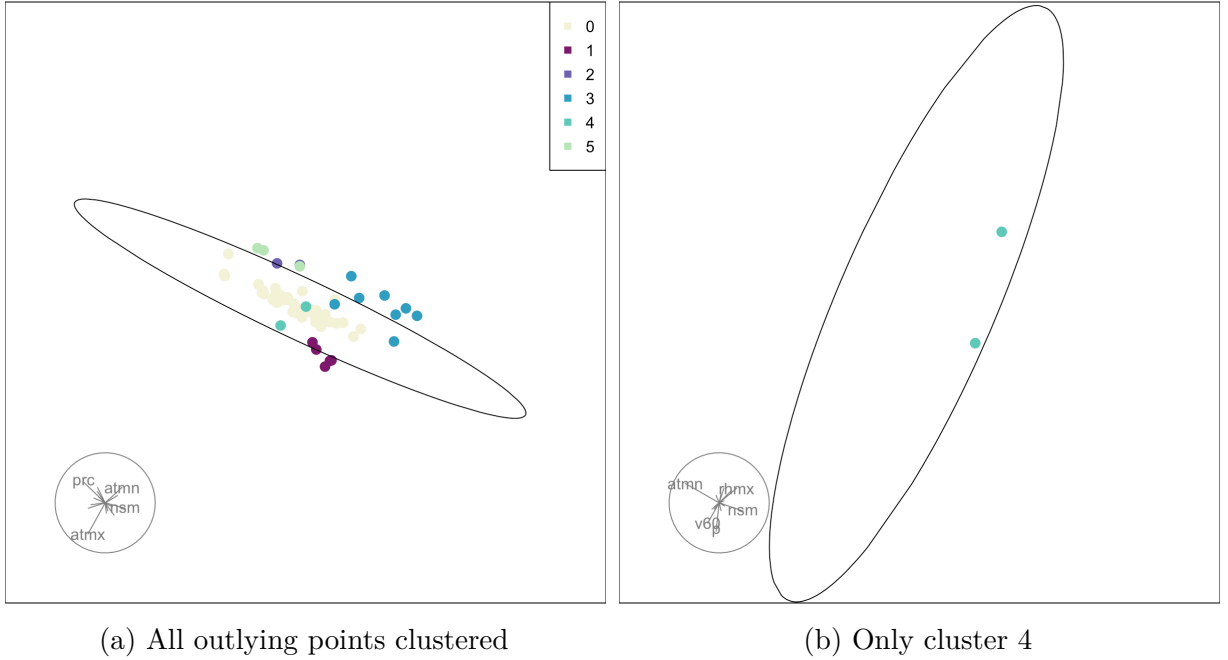


Figure 5: Examining weather anomalies using projections identified by the anomaly index: (a) computed on all outlying points, (b) computed only for cluster 4. In (a) the outlying points are somewhat orthogonal to the normal ellipse, which is primarily using the temperature min (`atmnn`) and max (`atmxx`) variables. In (b) the two observations are primarily extreme in the minimum temperature (`atmnn`) variable, and have lower than normal minima.

To compare our results to what is obtained by outlier detection methods, we reproduce one of the results from Filzmoser et al. (2018) in Figure 6. On top we can see the cluster assignments for all points that we have identified as outliers using the  $p$ -dimensional Mahalanobis distance.

For example we see that cluster 4 contains the years 1962 and 1996, and for these two years the result from Filzmoser et al. (2018) also indicates unusually low values for the minimum

temperature, while there is disagreement between outlyingness in other variables. Note that compared to the years 1965 and 1966 they have unusually low minimum temperature while having average values for the number of days with maximum temperature above 25°C, and this contrast is also captured in the projection.

When looking at the overall picture (Figure 5 (a)), we can see that the linear projection is showing the difference between minimum and maximum temperature, which is where clusters are outlying in different directions. The direction of cluster 1 is where the average maximum temperature is unusually higher compared to the minimum temperature, while clusters 3 corresponds to years where the minimum temperature is unusually close to the maximum temperature. This combined information cannot be resolved with the cell detection algorithm, but we see that for example the most recent years (cluster 3) were tagged for having unusually high values for both the minimum and the maximum temperature.

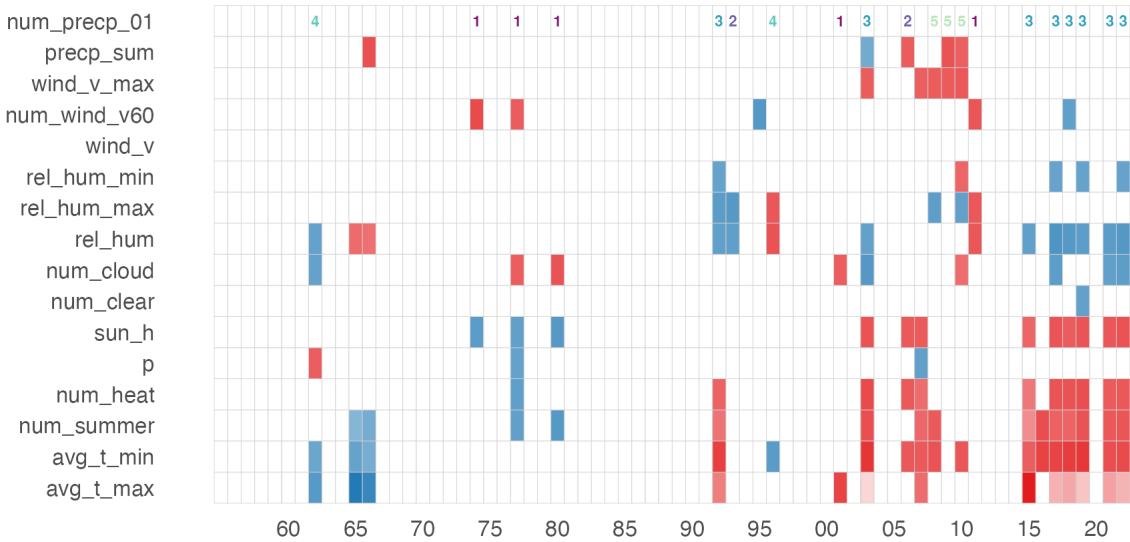


Figure 6: Reproduction of the results from [Filzmoser et al. \(2018\)](#), showing which cells have been identified as outlying by their Shapley Cell Detector algorithm. Red cells indicate values higher than expected, blue cells values lower than expected. For years that have been identified as outliers in our approach we show the cluster assignment at the top.

## 6 Conclusion

This paper has provided a new projection pursuit index for comparing a sample of data against a multivariate normal reference distribution. It has also provided an analytical result for drawing 2- $D$  projections of the  $p$ - $D$  ellipse corresponding to the normal reference distribution. These combined provide new ways to visualise multivariate data, for this particular scenario.

The work is related to outlier detection methods (see, [Filzmoser et al. 2018](#), for example), particularly those that use robust statistics, as illustrated in the weather example. Methods discussed in [Rousseeuw et al. \(2018\)](#) and [Donoho & Gasko \(1992\)](#) describe detecting outlyingness using projections of the data. When these projections are collected and used as a large set, they define a high-dimensional confidence region of an indeterminate shape. There is no analytical definition. However, we could explore the data relative to the high-dimensional shapes using the same approach described in [Section 2](#). You would generate points on the surface of the irregular shape, overlay the data on this to visualise with a tour.

The methods on directional outlyingness or Stahel-Donoho outlyingness, described above, lend themselves to new potential 1- $D$  projection pursuit indexes. These would integrate nicely into a 1- $D$  projection pursuit guided tour to interactively visualise the potential outliers relative to the rest of the sample.

Another potential direction of this work is with model-based clustering using Gaussian mixtures ([Fraley & Raftery 2002](#)), where ellipses form the basis of the model. Currently, the `mclust` software ([Scrucca et al. 2023](#)) has the capacity to show 2- $D$  ellipses for two variables, or axis parallel 2- $D$  ellipses for  $p$ - $D$ . The equations developed here for drawing

the 2- $D$  projection of a  $p$ - $D$  ellipse would provide more versatile visualisation for examining the model-based clustering fits.

## Acknowledgements

The work of first author Calvi was supported by the ResearchFirst undergraduate research program at Monash University. German Valencia advised on the project, in relation to physics applications.

The full paper, code and data to reproduce the work, are publicly available at [https://github.com/uschiLaa/anomaly\\_ppi](https://github.com/uschiLaa/anomaly_ppi).

## References

- Asimov, D. (1985), ‘The Grand Tour: A Tool for Viewing Multidimensional Data’, *SIAM Journal of Scientific and Statistical Computing* **6**(1), 128–143.
- Buja, A. & Asimov, D. (1986), ‘Grand Tour Methods: An Outline’, *Computing Science and Statistics* **17**, 63–67.
- Buja, A., Cook, D., Asimov, D. & Hurley, C. (2005), Computational Methods for High-Dimensional Rotations in Data Visualization, *in* C. R. Rao, E. J. Wegman & J. L. Solka, eds, ‘Handbook of Statistics: Data Mining and Visualization’, Elsevier/North-Holland, Amsterdam, The Netherlands, pp. 391–414.
- Cook, D., Buja, A., Cabrera, J. & Hurley, C. (1995), ‘Grand tour and projection pursuit’, *Journal of Computational and Graphical Statistics* **4**(3), 155–172.
- URL:** <https://www.tandfonline.com/doi/abs/10.1080/10618600.1995.10474674>

- Cook, D., Lee, E.-K., Buja, A. & Wickham, H. (2006), Grand Tours, Projection Pursuit Guided Tours and Manual Controls, *in* C.-H. Chen, W. Härdle & A. Unwin, eds, ‘Handbook of Data Visualization’, Springer, Berlin.
- Donoho, D. L. & Gasko, M. (1992), ‘Breakdown Properties of Location Estimates Based on Halfspace Depth and Projected Outlyingness’, *The Annals of Statistics* **20**(4), 1803 – 1827.
- URL:** <https://doi.org/10.1214/aos/1176348890>
- Filzmoser, P., Hron, K. & Templ, M. (2018), *Applied Compositional Data Analysis*, Springer, Cham, Switzerland.
- URL:** <https://doi.org/10.1007/978-3-319-96422-5>
- Fraley, C. & Raftery, A. E. (2002), ‘Model-based Clustering, Discriminant Analysis, Density Estimation’, *Journal of the American Statistical Association* **97**, 611–631.
- Friedman, J. H. & Tukey, J. W. (1974), ‘A Projection Pursuit Algorithm for Exploratory Data Analysis’, *IEEE Transactions on Computing C* **23**, 881–889.
- Gabriel, K. R. (1971), ‘The Biplot Graphical Display of Matrices with Applications to Principal Component Analysis’, *Biometrika* **58**, 453–467.
- Gower, J. C. & Hand, D. J. (1996), *Biplots*, Chapman and Hall, London.
- Halkidi, M., Batistakis, Y. & Vazirgiannis, M. (2002), ‘Clustering validity checking methods: Part ii’, *ACM SIGMOD Record* **31**.
- Hennig, C. (2024), *fpc: Flexible Procedures for Clustering*. R package version 2.2-12.
- URL:** <https://CRAN.R-project.org/package=fpc>
- Huber, P. J. (1985), ‘Projection Pursuit (with discussion)’, *Annals of Statistics* **13**, 435–525.



- Jones, M. C. & Sibson, R. (1987), ‘What is Projection Pursuit? (with discussion)’, *Journal of the Royal Statistical Society, Series A* **150**, 1–36.
- Lala, V., Zubair, M. & Minter, D. A. (2023), ‘Liver function tests’. Updated 2023 Jul 30.  
**URL:** <https://www.ncbi.nlm.nih.gov/books/NBK482489/>
- Lee, S., Cook, D., da Silva, N., Laa, U., Spyrisson, N., Wang, E. & Zhang, H. S. (2022), ‘The state-of-the-art on tours for dynamic visualization of high-dimensional data’, *WIREs Computational Statistics* **14**(4), e1573.  
**URL:** <https://github.com/dicook/wiley-isghdd>
- Maechler, M., Rousseeuw, P., Croux, C., Todorov, V., Ruckstuhl, A., Salibian-Barrera, M., Verbeke, T., Koller, M., Conceicao, E. L. T. & Anna di Palma, M. (2024), *robustbase: Basic Robust Statistics*. R package version 0.99-2.  
**URL:** <http://robustbase.r-forge.r-project.org/>
- Mahalanobis, P. C. (1936), ‘On the generalised distance in statistics’, *Sankhya A* **80 (Suppl 1)**, 1–7.  
**URL:** <https://doi.org/10.1007/s13171-019-00164-5>
- Rousseeuw, P. J. (1985), ‘Multivariate estimation with high breakdown point’, *Mathematical statistics and applications* **8**(283-297), 37.
- Rousseeuw, P. J., Raymaekers, J. & Hubert, M. (2018), ‘A measure of directional outlyingness with applications to image data and video’, *Journal of Computational and Graphical Statistics* **27**(2), 345–359.  
**URL:** <https://doi.org/10.1080/10618600.2017.1366912>
- Scrucca, L., Fraley, C., Murphy, T. B. & Raftery, A. E. (2023), *Model-Based Clustering*,

*Classification, and Density Estimation Using mclust in R*, Chapman and Hall/CRC.

**URL:** <https://mclust-org.github.io/book/>

Wickham, H., Cook, D., Hofmann, H. & Buja, A. (2011), ‘tourr: An R Package for Exploring Multivariate Data with Projections’, *Journal of Statistical Software* **40**(2).

**URL:** <http://www.jstatsoft.org/v40/i02/>

Wickham, H., Cook, D., Spyrison, N., Laa, N., Zhang, H. S. & Lee, S. (2024), *Tour Methods for Multivariate Data Visualisation*. R package version 1.2.0.

**URL:** <https://CRAN.R-project.org/package=tourr>